iJET EXPLORE International Journal of Engineering & Technology
CENTRE OF PROFESSIONAL RESEARCH PUBLICATIONS
ISSN 2049-3444

International Journal of Engineering and Technology Volume 2 No. 6, June, 2012

Dynamic Behaviour of an Electronically Commutated (Brushless DC) Motor Drive with Back-emf Sensing

O. Imoru, J. Tsado
Department of Electrical and Electronics Engineering,
Federal University of Technology, Minna, Nigeria

ABSTRACT

Conventionally, BLDC motors are commutated in six-step pattern with commutation controlled by position sensors. To reduce cost and complexity of the drive system, sensorless drive is preferred. The existing sensorless control scheme with the conventional back EMF sensing based on motor neutral voltage for BLDC has certain drawbacks, which limit its applications. This paper presents the dynamic behaviour of an analytical and circuit model of a Brushless DC (BLDC) motors with back emf sensing. The circuit model was simulated using LTspice and the results obtained were compared with the experimental results. The value of the motor constant and the back emf measured from the experiment agreed with the simulated model. The starting behaviour of the motor, changing of load torque when current are varied and disturbance of sensing method at peak load shows that the dynamic behaviour results of the experiment obtained from oscilloscope are similar to the simulated value.

Keywords: *BLDC, Dynamic behaviour, back-emf sensing, motor constant,*

1. INTRODUCTION

In numerous personal care appliances or domestic appliances an electro-mechanic driving system can be found, performing linear, rotational or vibrating movement [1-4]. One of the electro-mechanic driving systems is mostly used for these appliances is Brushless DC Motor. It is a type of electric motor which relies on an electronic controlled commutation. Conventional DC motors use a commutator in contact with a brush set to make the electrical contact which forms the electric current to the field coils windings. It uses an electronic controller which regulates and controls the voltage and current to the field coils and Brushless dc motors using a electronic controller requires a motor position sensor for the electronics to precisely determine and apply the correct signal timing. Some motors utilize a hall effect sensor to establish the position of the rotor relative to the field coils, however this hall effect sensor is expensive. Application of back emf sensor the detection of the motor's floating phase, which could be used to determine the commutation sequence without hall sensors. Application of back emf sensor is cheap and has also been found successful in some of the home appliances, automotive machine, audio loudspeaker and HVAC industry [6], however its application on BLDC motor has not been fully explore. Brushless DC (BLDC) motors are known for higher efficiencies, high torque to inertia ratios, greater speed capabilities, lower audible noise, better thermal efficiencies, lower EMI characteristics, compact form, high reliability and low maintenance [7-9].

The technique of commutation that is based on back-emf sensing is usually applied for rotational motor with a high rotational speed used in combination with a load that allows the motor to start up easily. This application can be found in a disk drive. However, the starting conditions can be very unfavourable in a case of a relatively low rotational speed application because of gear omission. This will cause the starting torque can be excessively high and it might prevent the motor from starting. The goal of this simulation model is to gain an insight in the above mentioned issues and to carry out a reliable driving concept. Finally severe peak loads are introduced to see the extent at which the commutation process is disturbed. An analytical modelling approach to determine the characteristics of Electronically Commutated (Brushless DC) Motor Drive with Back-emf Sensing using LTSpice (simulation model) has been varied experimentally in [10]. However the dynamic behaviour is presented in this paper and reveals better information about the best starting algorithms for the motor and its the response at peak load.

2. ELECTROMAGNETIC ACTUATOR

Details information on the Electromagnetic system (actuator) of a motor can be found [11-15]. The main focus of electromagnetic actuator is on rotational motors; however, the same approach can be followed for actuators performing a linear motion. The system is assumed to be linear which means the saturation or hysteresis effects are neglected. The relationship between N electrical inputs

(ports) and mechanical output (port) of an electromagnetic actuator in figure 1 are derived.

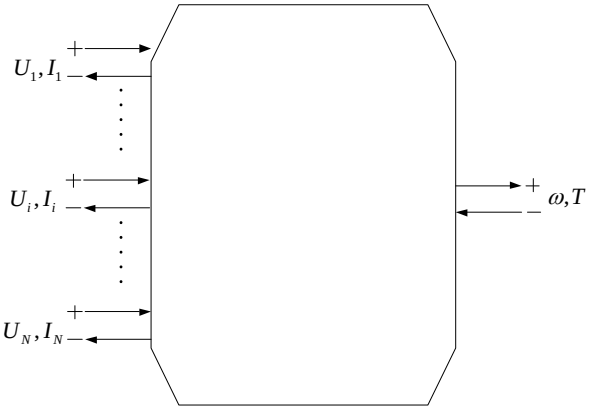

Figure 1: An electromagnetic system with N electrical ports and one mechanical port electromagnetic

The system converts electrical energy to mechanical energy and the mechanical domain is described with rotational parameters. The energy flows from electrical to mechanical side, however, the opposite energy flow i.e from mechanical to electrical side is also covered by the following derivation.

The flux though winding i generated by a winding j is:

$$\Phi_{ij} = \Lambda_{ij}(\alpha) F_j \tag{1}$$

Here, F_j is the ampere-turns through j and Λ, is the mutual permeance (i.e reciprocal of magnetic resistance called Reluctance) from winding j to winding i . This quantity depends on the rotor position.

Also

$$F_j = n_j I_j \tag{2}$$

where I is the current flowing in the winding j and *n* is the number winding in the port.

The total flux through winding i becomes

$$\Phi_i = \sum_{j=1}^{N} \Lambda_{ij}(\alpha) n_j I_j \tag{3}$$

And the voltage at the winding i is

$$U_i = n_i \frac{d\Phi_i}{dt} = n_i \frac{d}{dt}\left(\sum_{j=1}^{N} n_j I_j \Lambda_{ij}(\alpha) \right) \tag{4}$$

The total electrical input power therefore is

$$P_{el} = \sum_{i=1}^{N} U_i I_i = \sum_{i=1}^{N} n_i \frac{d}{dt}\left(\sum_{j=1}^{N} n_j I_j \Lambda_{ij}(\alpha) \right) I_i \tag{5}$$

Further expansion of equation (5) is

$$P_{el} = \sum_{i=1}^{N}\sum_{j=1}^{N} \begin{pmatrix} n_i n_j I_i I_j \frac{d\Lambda_{ij}(\alpha)}{d\alpha}.\omega... \\ +n_i n_j I_i \frac{dI_j}{dt} \Lambda_{ij}(\alpha) \end{pmatrix} \tag{6}$$

Where $\omega = \frac{d\alpha}{dt}$ is the rotor angular speed in rad/sec.

With equation (6), we know how much power supplied into the system and the corresponding extracted power at the mechanical side is

$$P_{mech} = \omega T \tag{7}$$

Where T is is the Torque generated.

The difference in the input and the output power corresponds with the increase of energy in the system. The energy in the system, W_{sys} is stored in the magnetic field produced by the system, thus, it is expressed as

$$W_{sys} = \sum_{i=1}^{N}\sum_{j=1}^{N} \left(\frac{1}{2} n_i n_j I_i I_j \Lambda_{ij}(\alpha) \right) \tag{8}$$

Then, the corresponding power with change in the system energy is

$$P_{sys} = \frac{dW_{sys}}{dt} = P_{el} - P_{mech} \tag{9}$$

Finding the derivative of equation (9) with respect to time, we have

$$P_{sys} = \frac{dW_{sys}}{dt} = \sum_{i=1}^{N}\sum_{j=1}^{N} \begin{pmatrix} \frac{1}{2} n_i n_j I_i I_j \frac{d\Lambda_{ij}(\alpha)}{d\alpha} \omega... \\ +n_i n_j I_i \frac{dI_j}{dt} \Lambda_{ij}(\alpha) \end{pmatrix} \tag{10}$$

From equations (6), (7), (9) and (10), we arrived at the expression for the Toque of the system in figure 1 as

$$T = \sum_{i=1}^{N}\sum_{j=1}^{N} \tfrac{1}{2} I_i I_j n_i n_j \frac{d\Lambda_{ij}(\alpha)}{d\alpha} \tag{8}$$

Thus, the electromagnetic system of figure 1 can be described by equations (4) and (8). The interaction between the electrical ports and the mechanical ports together with the magnetic coupling between the electrical ports are taken into account.

We shalll now consider a permanent magnet motor as shown in figure 2 to derive other relationships of the motor parameters

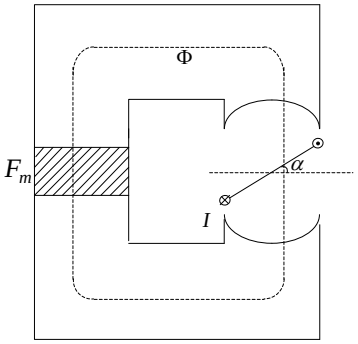

Figure 2: A permanent magnet Motor

A current carrying conductor placed in a permanent magnet electromagnetic system with a flux, $\Phi(Wb)$ having a cross-sectional area, $A(m^2)$, it experiences an mmf, $F_m(A)$. The magnetic flux density, $B(T)$ as a function of the rotor position is described as

$$\begin{aligned} \Phi_{1m}(\alpha) &= \Lambda_{1m}(\alpha)F_m = B_{1m}(\alpha)A_1 \\ \Phi_{1m}(\alpha) &= \hat{\Phi}_{1m}\cos(\alpha) = \hat{\Lambda}_{1m}\cos(\alpha)F_m = \hat{B}_{1m}\cos(\alpha)A_1 \end{aligned} \tag{9}$$

and $\Lambda_{1m}(\alpha) = \hat{\Lambda}_{1m}\cos(\alpha)$

Hence,

$$\begin{aligned} T &= \tfrac{1}{2} n_1^2 I_1^2 \frac{d\Lambda_{11}(\alpha)}{d\alpha} + \tfrac{1}{2} I_1 n_1 F_m \frac{d\Lambda_{1m}(\alpha)}{d\alpha} \\ &+ \tfrac{1}{2} F_m I_1 n_1 \frac{d\Lambda_{m1}(\alpha)}{d\alpha} + \tfrac{1}{2} F_m^2 \frac{d\Lambda_{mm}(\alpha)}{d\alpha} \end{aligned} \tag{10}$$

The first part of equation (10) represents the toque generated through the wind and the permanent magnet does not have any contribution to it. The second and the third part of the equation represent the torque used by the permanent magnet while the last is the torque due to cogging effect of the magnet.(The current through the winding has no effect on it)

The torque that is used by the permanent magnet is

$$\begin{aligned} T_{1m} &= I_1 n_1 F_m \frac{d\Lambda_{1m}(\alpha)}{d\alpha} = -I_1 n_1 F_m \hat{\Lambda}_{1m}\sin(\alpha) \\ &= -I_1 n_1 \hat{B}_{1m} A_1 \sin(\alpha) = -n_1 \hat{\Phi}_{1m}\sin(\alpha) I_1 = K(\alpha) I_1 \end{aligned} \tag{11}$$

This implies that the constant of proportionality, K is a function of the rotor position, α

3. CIRCUIT MODEL

As a result of the above derivations, motor equivalent-circuit with one electrical port (input) and one mechanical port (output) is formed in figure 3. The inductance of the winding are neglected while R is the winding resistance. The back emf is proportional to the speed of the rotor and similarly is torque to the current flowing in the winding. The motor constant (constant of proportionality) depends on the rotor position α [16-17]. Thus;

$$\begin{aligned} T &= K(\alpha) I_1 \\ U &= K(\alpha)\omega \end{aligned} \tag{12}$$

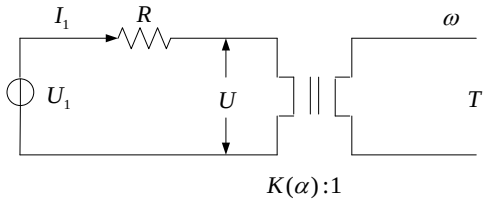

Figure 3: Simple circuit-diagram of winding resistance and motor constant

Figure 3 is incomplete because the eddy current has not been included in the model. Therefore, figure 4 shows an improved model of figure 3. The torque source T_c represents the coulomb friction whose sign is dependent on the direction of the motor axis. In figure 4, we assume that the motor rotates in only one direction; therefore this fractional torque is positive and constant. For simplicity we assume that this frictional torque is present, even when the rotor speed is zero.

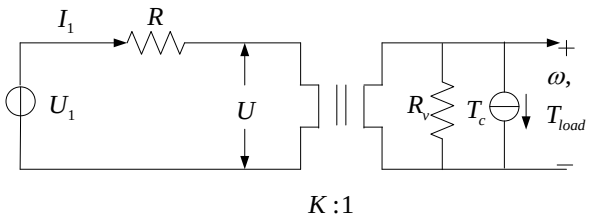

Figure 4: Circuit-diagram of motor an improved figure 3

There is also a resistance, R_v to the rotational speed. The motor constant was first determined in other to find the frictional parameters, T_c and R_v, before the behaviour of the motor. The load torque T_{load} and the summation of the Frictional torques T_{fr} are proportional to the input current I_1, with motor constant of proportionality, K as described by the equation below

$$T_{load} = K \bullet I_1 - T_{fr} = K \bullet I_1 - \frac{\omega}{R_v} - T_c \qquad (13)$$

The frictional parameters T_c and R_v were also estimated in a similar way with the proportionality constant.

4. EXPERIMENTS

The characteristics of the motor are first predicted in other to validate the measured parameters. In doing this, a simulated circuit model in LSpice program is used. Since the new motor commutate by back emf sensing, the configuration of commutation sequence is consider based on M6R9 (i.e a 6 pole pair of the permanent magnet motor containing 9 winding poles in the stator) [18]. The back emf is proportional to the rotational speed and the same constant of proportionality is related to Toque-Current characteristics. The motor constant was first predicted from the data generated by the circuit model.

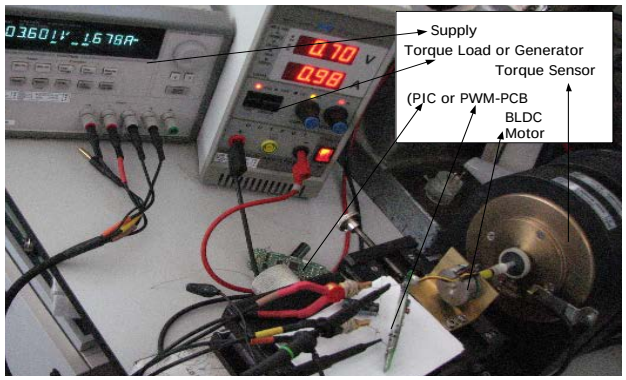

Figure 5: Measurement set-ups with Torque sensing machine to determine BLDC motor behaviour

A printed circuit board (PCB) of either pulse-width modulation (PWM) or Peripheral Interface Controller (PIC) can be used to drive such motor. The PWM PCB is an uncontrolled speed board while the PIC PCB is a speed control board. In this experiment, a voltage of 3.6V is supply via a PCB (PWM with 91% duty cycle) was used to drive the motor in before it is being loaded gradually (figure 5). Measurements of the speeds and currents are made at each load given to the motor. The dynamic behaviour of the motor is also observed at peak load.

5. DISCUSSIONS OF RESULTS

The back emf data obtained from the experiments were used in the simulation model. The comparison of the back emf against speed for both experiment and simulation are shown in figure 6

The motor constant, K obtained from the simulated model is $K_{sm}=7.459\times10^{-3}$Nm/A while the motor constant obtained from the experiment (figure5) is $K_{em}=7.337\times10^{-3}$ Nm/A. The values of frictional parameters T_c and R_v obtained from the simulation model and the experiment are:

Frictional Parameters:

$$T_{csm} = 9.864\times10^{-4}\text{Nm},\ R_{vsm}=4.733\times10^{5}\text{rad/A/N/m}$$

$$T_{em} = 5.254\times10^{-4}\text{Nm},\ R_{em}=7.297\times10^{5}\text{rad/A/N/m}$$

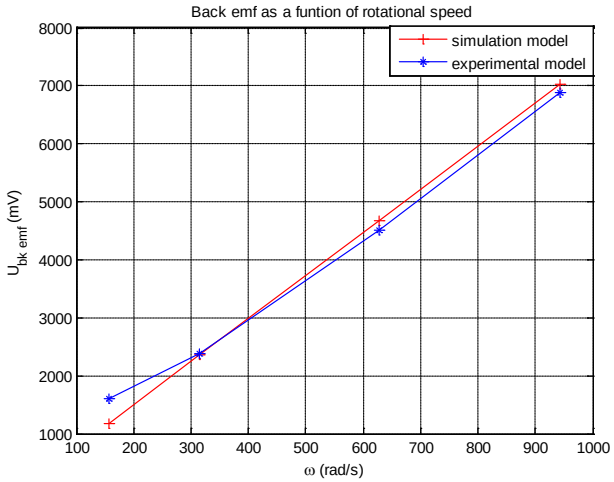

Figure 6: Back emf comparison of experimental and simulated models against rotational speed

The experimental results of the average current and peak to peak value of the back emf $U_{bk\ emf\,(pp)}$ from screen of oscilloscope were compared with the LTSpice simulated results at a nominal toque load of $5\times10^{-3}\,Nm$ and later at a peak toque load of $20\times10^{-3}\,Nm$. Figures 7 and 8 respectively present these comparisons. From the two figures, it implies that the sensing method is disturbed in both simulated and experimental results at peak load as shown in figure 8.

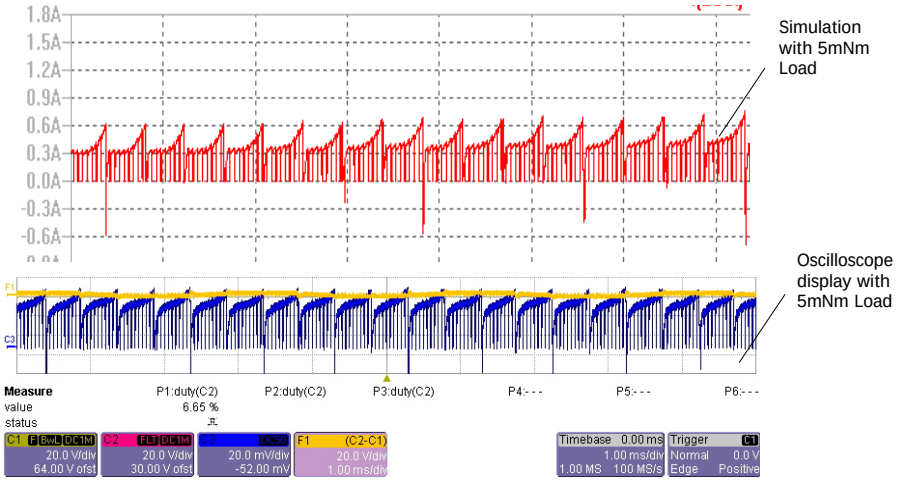

Figure 7: Current view of simulation and oscilloscope with Toque load 5mNm

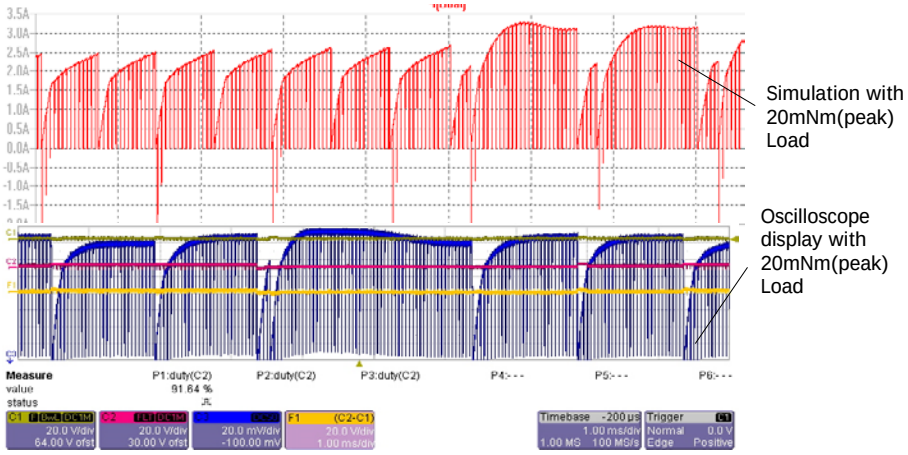

Figure 8: Current view of simulation and oscilloscope at 20mNm (peak) Load

Furthermore, when the motor is operating at a speed of 6000 rpm (i.e about 630 rad/s), the back emf of both experiment from screen of oscilloscope were compared with the LTSpice simulated results as shown in figure 9.

The peak to peak experimental value of the back emf $U_{bk\ emf\ (pp)}$ from screen of oscilloscope was 5.2V while 5.4V was obtained from the LTSpice simulation model.

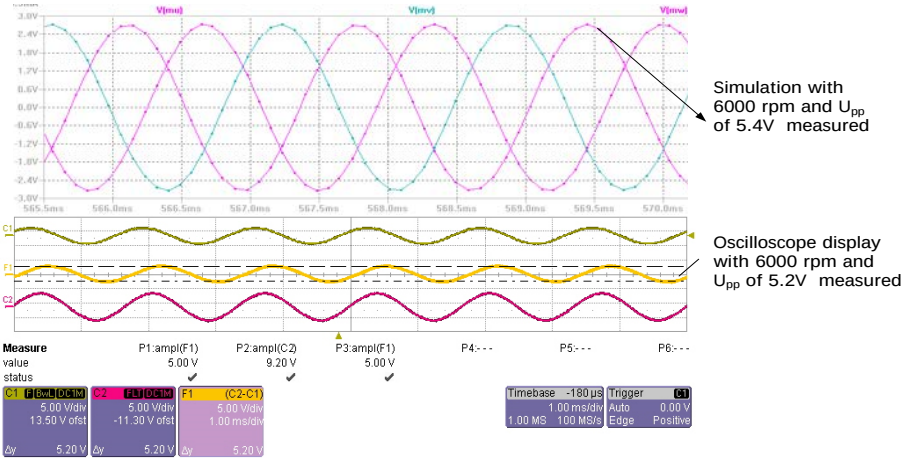

Figure 9: Back emf view of simulation and oscilloscope with 6000rpm speed

6. CONCLUSIONS

The dynamic behaviour of an electronically commutated (Brushless DC) Motor Drive with Back-emf Sensing has been carried out successfully. For a good modelling, the motor constant from the simulation using experimental parameters is expected to be more than 95% accuracy [17] and the motor constant obtained from the experimental results of this paper is 98.3% accuracy. Thus Measurements made validates the Circuit model. However, the discrepancies in measured value of frictional parameters in section 5 imply that the simulated model with higher frictional torques requires more currents at no load while the current obtained from the experimental model is lower due to the lower frictional torques. The value of T_c and R_v could be different if another BLDC motor is used in the experiment. The dynamic behaviour results obtained from the experiment are similar to the ones from the LTSpice simulation.

ACKNOWLEDGEMENT

The experimental study was done at Philips Consumer Lifestyle AT-Drachten in The Netherlands during my internship. The authors would like to thank the Internship supervisor for his advice, support, motivation and the provision of material needed for the experiment.

REFERENCES

[1] T. Szolc and A. Pochanke, "Transient and steady-state coupled electromechanical vibrationanalysis of the micro-drive system" XXIV Symposium *Vibrations in Physical Systems*, Poznan – Bedlewo, May 12-15, 2010

[2] C. Lin, H. Jan and N. Shieh, "GA-Based Multiobjective PID Control for a Linear Brushless DC Motor" IEEE/ASME Transactions on Mechatronics, Vol. 8, No. 1, March 2003, pp96-65

[3] Dunfield et al., "Position Detection for a Brushless DC Motor with hall effect device using a mutual inductance dectection method" U S patent, Number 5254914, Oct. 1993

[4] P. Yedamale, "Brushless DC (BLDC) Motor Fundamentals (AN885), "Microchip Tecnology Inc., 2003. [Online]. Available: http://www.jimfranklin. info/microchipdatasheets/00885a.pdf. [Accessed: Feb.12, 2012].

[5] T. Szolc et al, "An Application of the Magneto-Rheological Actuators to Torsional Vibration Control of the Rotating Electro-Mechanical Systems", Proceedings of the 8th IFToMM International Conference on Rotordynamics, September 2010

[6] J.Shao, D.Nolan, and T.Hopkins, "A Novel Direct Back EMF Detection for Sensorless Brushless DC (BLDC) Motor Drives," Applied Power Electronic Conference (APEC 2002), pp33-38

[7] D. M. Erdman, "Control system, method of operating an electronically commutated motor, and laundering apparatus," US Patent 4654566, March 31, 1987.

[8] T.Endo, F.Tajima, et al., "Microcomputer Controlled Brushless Motor without a Shaft Mounted Position Sensor," IPEC-Tokyo, 1983.

[9] K.Uzuka, H.Uzuhashi, et al., "Microcomputer Control for Sensorless Brushless Motor ," IEEE Trans. Industry Application ,vol.IA-21, May-June, 1985.

[10] O. Imoru, J.Tsado "Modelling of an Electronically Commutated (Brushless DC) Motor Drives with Back-emf Sensing" *IEEE Mediterranean Electrotechnical Conference (MELECON),* March 2012, Pg 828-831

[11] Sung-Q Lee, Dae-Gab Gweon., "A new 3-DOF Z-tilts micropositioning system using electromagnetic actuators and air bearings," Precision Engineering, Volume 24, Issue 1, January 2000, Pages 24-31

[12] L. Kather et al, "Method of adjusting the position of rest of an armature in an electromagnetic actuator" US Patent 5804962, Sept., 1998.

[13] G. Bergstorm, "System for control of an electromagnetic actuator." US patent 6249418, Jun. 19, 2001

[14] J. Seale et al, "Syetm and method for servo control of nonlinear electromagnetic actuator," US patent 6208497, March. 27, 2001

[15] J. Melbert, A. Koch, "Sensorless Control of Electromagnetic actuator for variable valve train., SAE International, 2000

[16] A. Lumsdaine, J. H. Lang, and M. J. Balas, "A state observer for variable reluctance motors: Analysis and experiments," in Proc. Incremental Motion Contr. Syst. Symp., June 1986, pp. 267-273.

[17] P. C. Sen, Principles of Electric Machines and Power Electronics,*John wiley & Sons Inc., 2nd ed,* 1997, pp 102-115

[18] http://www.mitsumi.co.jp/latest/Catalog/compo/motorav/index_e.html

AUTHORS' BIOGRAPY

'Ayo IMORU obtained his MSc in Electrical Engineering at Delft University of Technology, The Netherlands in 2010. He got his B.Eng. in Electrical and Computer Engineering with a First Class Honours and the overall best students from Federal University of Technology, Minna, Nigeria in 2005. His brilliance earned him an automatic employment as an Assistant Lecturer in the same department he graduated after his mandatory one-year (NYSC) National Youth Service Corps in 2007. He is a member of IEEE and SPE. His research interests include Electrical Machine, Power System and Energy Studies/Smart grids, Power Electronics and Drives.

Jacob Tsado Received is Bachelor of Engineering (**B. Eng**.) in Electrical /Computer Engineering from Federal University of Technology Minna, Nigeria in 1998. He received M.Eng and P.hD in Power System & Machine from University of Benin, Benin city, Nigeria in 2001 and 2007 respectively. Presently he is lecturing in the Department of Electrical Electronics, Federal University of Technology Minna, Nigeria. He is a member of IEEE, the councillor of student members IEEE. A member of Nigerian Society of Engineers and COREN register. His research area is power system and energy studies.